Journal of Rock Art (JRA)

DOI:http://doi.org/10.65098/jra.02.2025.01.10

E-ISSN: 2976-2421
CODEN: JRAOCQ

RESEARCH ARTICLE

ASSESSING WEATHERING DAMAGE TO HELANKOU ROCK ART BY INTEGRATING MORPHOLOGICAL AND IN-SITU PERFORMANCE DATA

Xiaotong Huo[1, 2], JiaWang[1, 2], Shu Jiang[3], Jianping Li[4], Erna Ma[4], Jinhua Wang[5*]

[1] Shaanxi History Museum, Xi an 710061, China
[2] Key Scientific Research Base of Conservation & Restoration for Mural as Collection and Materials Science in State Administration for Cultural Heritage
[3] School of Design, Shanghai Jiao Tong University, Shanghai 200240, China
[4] Yinchuan Municipal Administration of Helan Mountain Rock Art, Yinchuan 750001, China
[5] Department of Cultural Heritage and Museology at Fudan University, Shanghai 200433, China

** Corresponding Aauthor Email: jinhuawang@fudan.edu.cn*

ARTICLE DETAILS

Article History:

Received 26 Sep 2025
Accepted 20 Oct 2025
Available online 28 Nov 2025

Online Article Code

ABSTRACT

Assessing weathering damage to rock art requires a holistic understanding of physical degradation mechanisms and their environmental drivers. Static morphological assessments focus on visible symptoms of damage, whereas dynamic performance-based assessments examine intrinsic properties. However, these assessments remain disconnected. Moreover, traditional survey methods reflect the extent of weathering effects but fail to effectively evaluate stability. Therefore, this study used an integrated approach combining morphological observations and in-situ nondestructive performance data to evaluate the deterioration of Helankou rock art. Leeb hardness testing, thermal imaging, moisture measurements, and ultrasonic wave velocity analyses were conducted. Correlation analyses were used to examine the relationship between the structural deterioration and internal rock quality. In addition, a dynamic deterioration model was developed for the temporal evolution of weathering. Furthermore, multiple-criteria decision-making methods were used to quantify the relative importance of weathering criteria. The results revealed significant mechanical weakening in areas subject to splitting and blistering associated with internal voids and fissures. Thermal and hydrological anomalies associated with these defects accelerated weathering through increased thermomechanical stress and moisture retention. The rock quality index was validated as an effective metric for quantifying deterioration extent. The results identified the progressive evolution from latent fissures to active splitting and irreversible delamination. Splitting was the most critical hazard, which could guide future conservation prioritization. This study highlights the importance of continuous environmental monitoring and advanced diagnostic techniques for supporting sustainable rock art preservation. Moreover, this integrated methodology provides a transferable framework for assessing and managing rock art deterioration.

KEYWORDS

Cultural Heritage Conservation, Rock Art Deterioration, Integrated Assessment

1. INTRODUCTION

Immovable stone heritage, a testament to human civilization, faces severe global conservation challenges. Extreme climatic conditions, such as drastic temperature fluctuations and freeze-thaw cycles, significantly accelerate the weathering of sandstone artifacts, particularly in cold and arid regions, such as northern China (Huo et al., 2024). Helankou rock art is a vital cultural heritage site of ancient rock art in China, and its current state of preservation is a matter of urgent concern.

The evaluation of stone monument damage has historically relied on qualitative descriptions and morphological classifications. The field has undergone a significant transformation beginning in the late 1970s. Early efforts focused on establishing universal terminology to describe weathering phenomena, thereby providing a common language for conservation professionals worldwide (Siedel & Siegesmund, 2014). Subsequent research built on this foundation, developing more refined classification systems and quantitative assessment methods (Fitzner et al., 1997, 2002), such as the damage index (Fitzner et al., 2003, 2004; Randazzo et al., 2020). This evolution effectively integrated the static characteristics of weathering, that is, its form and extent, into a measurable academic framework, standardizing in-situ investigations and data recording.

Despite the significant progress in traditional morphological surveys using static assessments, their inherent limitation lies in their inability to reveal the underlying mechanisms and future trends of weathering. Although these methods quantify the current state of decay, they fail to answer critical questions, such as the reason that damage is occurring, the rate at which damage is progressing, and the structural integrity of the stone. In contrast, dynamic assessment methods that use nondestructive testing (NDT) to obtain mechanical and physical parameters of the rock material directly reflect the performance degradation of the stone body (Leucci & Giorgi, 2022). Weathering alters rock composition and microstructure. Many studies have found a strong correlation between rebound strength and mechanical properties, such

as elastic moduli (Desarnaud et al., 2019; Si-jian et al., 2021). Research has shown that ultrasonic pulse velocity is a reliable indicator of internal flaws, including cracks, voids, and density changes, that are often not visible on the surface but are critical for assessing structural health (Menningen et al., 2018; Siegesmund et al., 2021).

The fundamental research gap lies in the disconnect between these two assessment approaches, namely, static morphological assessments that focus on visible symptoms and dynamic performance-based assessments that examine intrinsic properties. Traditional survey methods predominantly reflect the extent of the impact of weathering but fail to effectively evaluate the state of stability. This study aimed to bridge this gap by integrating static morphological data with dynamic performance data into a unified evaluation framework. Combining these two types of information provides a comprehensive understanding of the damage caused by weathering and a scientific basis for developing targeted conservation strategies.

This study aimed to establish a comprehensive damage assessment framework and implement it to explore complex weathering issues in Helankou rock art. The proposed framework systematically integrates the extent of impact (based on the damage index) and state of stability (based on NDT performance data). Furthermore, this study used the analytic hierarchy process (AHP) and fuzzy comprehensive evaluation (FCE) to quantify these factors and achieve a holistic and actionable assessment of weathering damage. This approach elevated this study from a simple case analysis to that offering a methodological contribution with broad applicability.

2. MATERIALS AND METHODS

2.1 Study Area and Geological Setting

Helankou rock art, a representative system of northern Chinese rock art, is located in the eastern foothills of Helan Mountains in Helan County, Yinchuan City, Ningxia Hui Autonomous Region, China. Based on the geomorphological and environmental characteristics, the site is distributed across six sectors (A-F; Figure 1). Mountainous rock art predominantly occurs in sectors B and C. This study surveyed 190 rock art panels at 14 sites (B1-B14) in Sector B and 337 panels at 21 sites (C1-C21) in Sector C. The rock panels were typically situated 1-5 m above the valley floor, with some instances as high as 20 m. Comprehensive studies on the assessment of rock art deterioration, encompassing field investigation, classification of damage types, and damage index analyses, have been presented in prior publications (Huo et al., 2024); hence, they are not reiterated here.

2.2 Evaluation Methods

A comprehensive assessment framework was established by integrating data from NDT with FCE using factor weights determined by the AHP. This approach allowed robust multiple-criteria decisions regarding complex weathering issues.

The AHP, developed by Saaty (1983), is a multiple-criteria decision-making method that combines qualitative and quantitative information by organizing complex problems into a hierarchical structure (Olson, 1996). This study used the AHP to quantify the relative importance of various weathering criteria. The procedure involved constructing a hierarchical structure of assessment goals and criteria using Saaty's (1983) nine-point scale for pairwise comparisons, calculating weights from the principal eigenvector of the judgment matrix, and verifying consistency using the consistency ratio (CR).

FCE is a robust method for handling ambiguity and diverse criteria by quantifying the membership degrees of the evaluation objects within fuzzy sets. This method was used to integrate the severity and stability factors of weathering damage into a fuzzy evaluation matrix. By leveraging fuzzy mathematics, FCE converts subjective assessments into numerical calculations, providing nuanced and comprehensive assessments that account for the uncertainties inherent in the evaluation of complex natural phenomena (Xu et al., 2023).

2.3 NDT

Several complementary in-situ NDT techniques were employed to characterize weathering-induced degradation of Helankou rock art (Figure 2). The major advantage of NDT is its capacity to assess, diagnose, and monitor the condition of rock art without compromising its stability or authenticity, while offering portability, efficiency, and the capability for non-contact large-scale surveys (Bodnar et al., 2012; Tejedor Herrán et al., 2024).

Mechanical degradation was quantified using the Leeb hardness test.

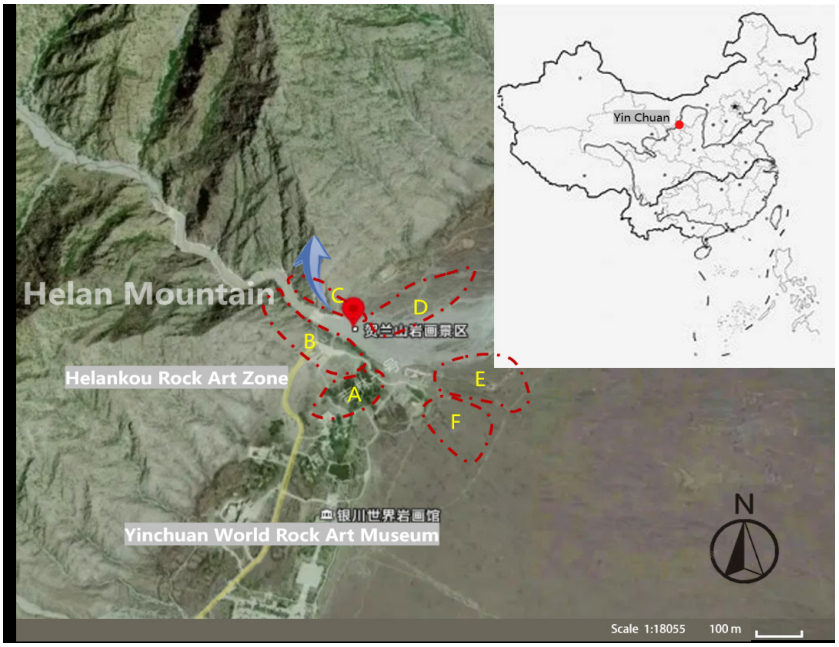

Figure 1 Distribution Map of Helankou Rock Art

Figure 2 Photographs of in-Situ Testing Methods at Helankou: (a) Leeb Hardness Test Conducted on July 30, 2022; (b) Microwave Moisture Measurement Conducted on February 18, 2022; (c) Infrared Thermography Test Conducted on July 18, 2021; (d) Surface Temperature Test Conducted on July 18, 2021.

This method calculates a hardness number (HLD) based on the rebound velocity relative to the impact velocity of a spring-driven body (Wilhelm et al., 2016). Measurements were conducted using a Proceq Equotip device equipped with a D probe, which was selected due to its shallow impact depth and high sensitivity. To avoid micro-damage to the cultural heritage, the single impact method was adopted instead of the repeated impact method (Desarnaud et al., 2019).

Moisture content was assessed using a handheld HF Sensor Moist 210, which probes to a depth of 2-3 cm. To convert the semi quantitative device readings into accurate moisture data, a gravimetric calibration was performed on representative rock samples (Dario Camuffo, 2018). In addition, infrared thermography and microwave moisture measurements were conducted at all positions to comprehensively assess variations in surface temperature and moisture content across rock art panels.

Infrared thermography for thermal and moisture mapping was used to capture thermal variations on the rock surfaces (Davin et al., 2017). A Testo 890 infrared camera, operating in a passive thermography mode, was employed to obtain the natural temperature differences caused by solar heating and cooling cycles.

Three positions were selected within the test area for in-situ testing: Position 1 represented the intact rock surface, used as a reference for undamaged areas; Position 2 corresponded to blistering or near-splitting zones with visible voids between the surface layers and bedrock; and Position 3 comprised areas with spalled off surface rock, exposing the subsurface bedrock (Figure 3).

In-situ ultrasonic pulse velocity measurements were performed using a Proceq Pundit instrument with a 54 kHz P wave exponential sensor probe, 10 cm spacing, 300 V voltage, and 10 X gain (Figure 4). Based on the observed damage distributions, two types of measurement points with combined blistering and splitting exceeding 15% were selected. Type AB points were located in areas with evident splitting or blistering and used to measure pulse velocity (Vm_{AB}), whereas Type BC points were located in the adjacent sound bedrock and served as control measurements (Vm_{BC}).

2.4 The Rock Quality Index (QI)

The rock quality index (QI) is used to assess rock mass porosity by comparing elastic wave velocities (Fourmaintraux, 1975). It is defined as the ratio of the measured wave velocity (V_m) to the theoretical velocity (V_c) of an ideal defect-free rock (Siegesmund et al., 2021; Xu et al., 2024; Young-Jun Lee et al., 2012), as follows:

$$QI = \frac{V_m}{V_c} \times 100\%$$

A lower QI indicates a larger difference between measured and theoretical velocities, reflecting a large number of internal voids, fissures, and pores and signifying poorer rock quality.

V_c is calculated based on the rock's elastic properties (Pappalardo, 2015) following Aleksandrov's (1933) theory, which averages mineral elastic moduli and proportions. V_c is always higher than V_m because ideal rock has no defects. The relationship between V_c, Young's (1807) modulus E, Poisson's (1837) ratio μ, and density ρ is

$$V_c = \sqrt{\frac{E(1-\mu)}{\rho(1+\mu)(1-2\mu)}}$$

For the Helankou rock mass, E = 3.288 × 104 MPa, μ = 0.195, and ρ = 2670 kg/m^3; thus, $V_c \approx$ 4377.68 m/s. This method represents in-situ conditions better than laboratory tests because it accounts for natural

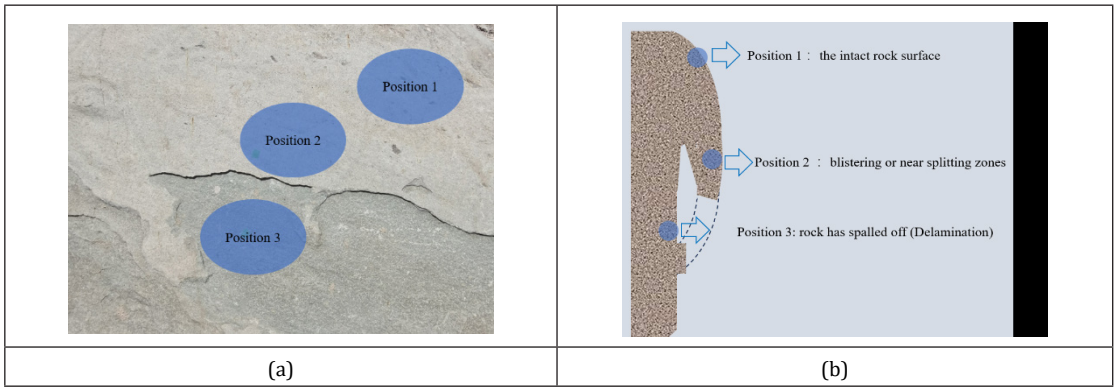

Figure 3 Schematic Diagram of in-Situ NDT Positions: (a) Plan View; (b) Cross-Sectional View Illustrating the Distinctions Between the Positions.

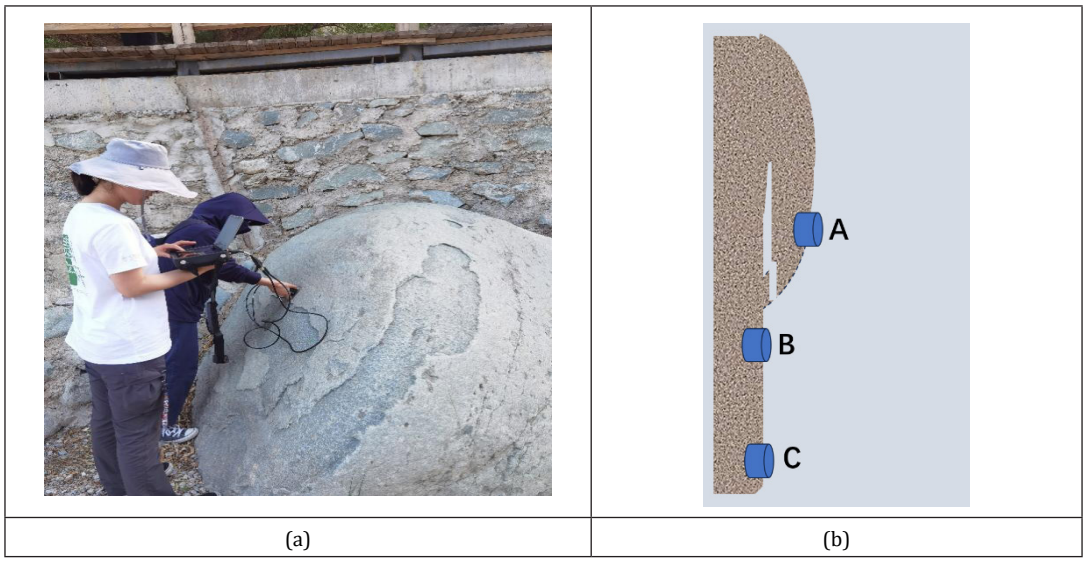

Figure 4 In-Situ Wave Velocity Measurements: (a) Photograph; (b) Schematic Diagram of Wave Velocity Measurement Positions.

rock variability.

3. RESULTS

3.1 In-Situ Nondestructive Physical Property Measurements

3.1.1 Leeb Hardness Test Results

As shown in Table 1, the coefficient of variation (CV%) indicated good data consistency across all test positions. Statistically significant differences in mean hardness were observed among the positions (Figure 5). The non-deteriorated area exhibited the highest average hardness value (626 HLD), whereas the blistering area showed the lowest average hardness value (535 HLD), reflecting the impact of deterioration on surface mechanical properties. Low hardness values directly corresponded to the loss of kinetic energy during impact, which was a function of the plastic deformation of the rock and a reliable indicator of reduced mechanical strength.

3.1.2 Surface Temperature and Moisture Content Analyses

As shown in Table 2, the average surface temperature in blistering and splitting zones (32.2°C) was higher than that in non-deteriorated (30.5°C) and post-delamination subsurface (30.1°C) areas. The temperature differential between the rock art surface and rock cavity was approximately 2°C. This thermal anomaly was a key symptom of subsurface voids, as the air trapped within these cavities acted as a thermal insulator, preventing heat dissipation and causing the temperature in the surface layer to increase.

Moisture content analyses revealed relatively high surface moisture in the non-deteriorated area (approximately 2%) and low and consistent surface and internal moisture levels in the post-delamination subsurface area (0.47–0.77%; Table 3). Notably, the blistering area exhibited a high surface moisture content (up to 4.2%) despite the low internal moisture content (approximately 0.5%). This indicates that these voids and fissures act as moisture reservoirs, accumulating and retaining water from precipitation.

Temperature and moisture measurements were obtained under varied environmental conditions (summer vs. winter), limiting direct

Table 1 Leeb Hardness Test Results at Various Positions

Test Position	Number of Valid Tests (N)	Mean Hardness (HLD)	Coefficient of Variation (%)
1	24	626	18.7
2	31	535	20.9
3	23	569	21.2

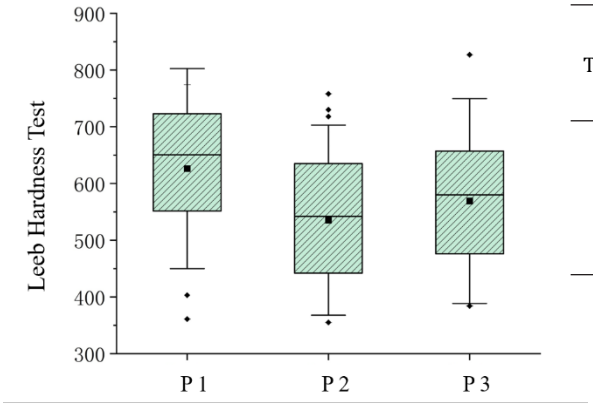

Figure 5 Box Plot of Leeb Hardness Test Values

comparison. However, they served as useful relative indicators that identified the rock's response to specific environmental stresses.

3.1.3 Field Wave Velocity Testing and Rock Quality Index

In this study, QI_i values were calculated by comparing the ultrasonic wave velocities on paths with voids (Vm_{AB}) and void-free paths (Vm_{BC}). Using in-situ bedrock velocity as a background improved accuracy. As shown in Table 4, higher QI_i values were correlated with more voids and severe deterioration, whereas lower values indicated denser and less damaged rock.

To quantitatively assess the relationship between structural deterioration and internal rock quality, a linear regression model was used to describe the relationship between deterioration coverage and QI_i (Figure 6). The analysis yielded a Pearson correlation coefficient of r = 0.82 (p = 0.004), indicating a statistically significant and strong positive linear relationship. This suggested that areas with higher QI_i values corresponded to greater deterioration coverage, providing a quantitative basis for predicting susceptibility to active damage.

3.2 Static and Dynamic Characteristics of Deterioration

3.2.1 Static Deterioration

In-situ observations revealed a concentric delamination pattern

Table 4 In-Situ Wave Velocities and Rock Quality Indices for Selected Areas of Helankou Rock Art

Rock Art No.	Splitting and Blistering	Vm_{AB} m/s	Vm_{BC} m/s	Rock Mass Quality Difference QI_i
B1	25.5	1754	2439	0.248
B2	14.55	2005	2500	0.113
B4	14.98	1849	3229.1	0.133
B5	13.73	2344	2891.25	0.125
B6	17.02	1829	2809	0.224
C5	15.1	2873	3333	0.105
C7	23.8	2238	3094.8	0.196
C10	23.1	2742	3632	0.203
C12	15.07	2913	3298.5	0.0884
C16	21.87	18634	2431	0.267

Table 2 Surface Temperature Test Results

Test Position	Number of Valid Tests (N)	Mean Temperature (°C)	Maximum Temperature (°C)	Minimum Temperature (°C)	Standard Deviation
1	24	30.5	39.1	26.2	4.08
2	31	32.2	44.1	28.0	3.47
3	23	30.1	40.0	25.8	4.19

Table 3 Surface Microwave Moisture Test Results

Test Position	Number of Valid Tests (N)	Moisture Content 2–3 cm (%)	Moisture Content 20–30 cm (%)
1	4	2.0	0.87
2	4	4.2	0.50
3	4	0.77	0.47

progressing inward from the outer surface, with delamination layers ranging from 2 to 11 mm in thickness (Figure 7). Crack measurements characterized large cracks averaging 80 mm in length and 10 mm in width (Figures 8 and 9). The morphology of the weathered material varied from angular blocks (3-14 cm) to sheet-like fragments (Figure 10). The deterioration was mainly concentrated in the superficial 0-10 mm zone, with delamination leading directly to a severe loss of rock art information. Quantitative assessment of the degree of impact revealed that delamination exerted the greatest impact, whereas splitting and blistering had a minor impact on the visual preservation of rock art (Table 5).

3.2.2 Dynamic Deterioration

Integrating in-situ observations and characteristic analyses of weathering deterioration indicated that the surface development of Helankou rock art was a progressive and irreversible process A spherical surface-deterioration model was employed to illustrate three stages of development(Figure 11): (1) an initial stage with no visible deterioration morphology; (2) a developmental stage characterized by fissure expansion, local bulging, and partial loss of iconographic information due to blister rupture; and (3) a final stage with extensive blistering and splitting culminating in surface delamination and complete loss of surface details. This model highlighted the dynamic nature of weathering and provided insights into the mechanisms governing the deterioration of the Helankou.

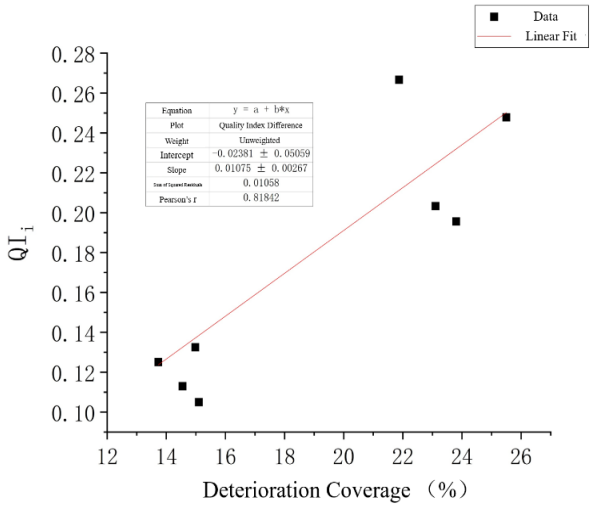

Figure 6 Linear Regression Between Deterioration Coverage and QI_i

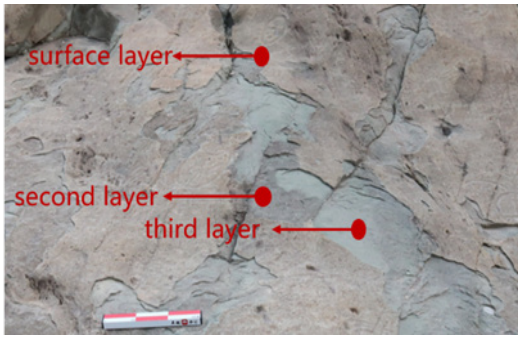

Figure 7 Schematic Diagram of the Delamination Sequence of Weathered Layers

Figure 8 Schematic Diagram Showing Features of Blistering and Splitting

Figure 9 Schematic Diagram of Geometric Parameter Measurements of Splitting

Figure 10 Schematic Diagram of Sheet-Like Detachment Morphology

Table 5 Quantitative Assessment of Deterioration Impact

Deterioration Type	Total Area (%)	Weathering Type Parameter	Deterioration Impact	Normalized Value
Blistering	0.02	4	0.08	0.065
Splitting	0.05	4	0.2	0.163
Delamination	0.19	5	0.95	0.772

We analyzed the stability of blistering, splitting, and surface delamination deterioration based on the development model of surface weathering deterioration in Helankou rock art. Blistering and splitting deterioration were in the development stage, whereas local bulging deformation and fissures continued to expand, rendering them highly unstable and increasing the risk of deterioration. Surface delamination deterioration was in the final stage of weathering. After the unstable surface layers peeled off, fresh bedrock and the delamination morphology were exposed, leading to a stable state.

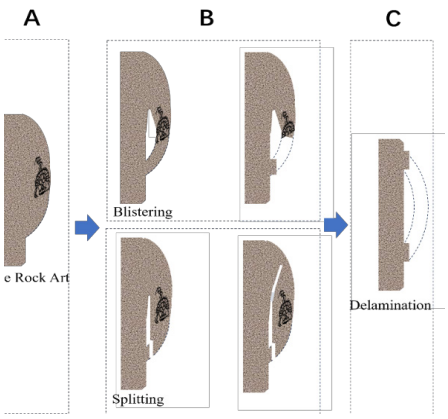

Figure 11 Schematic Model of Surface Weathering Deterioration Development in Helankou Rock Art

3.3 Quantitative Assessment of Deterioration Stability

The AHP was employed to quantitatively evaluate the stability of three types of rock art deterioration: blistering, splitting, and delamination. Four key indicators—surface thickness, crack length, surface hardness, and wave velocity—were used to construct a judgment matrix based on their relevance to the static and dynamic characteristics of deterioration and their potential effects on rock art stability.

Surface thickness reflected the depth of the damage of surface pathologies, such as cracking and spalling, and served as an important parameter for quantifying deterioration severity. Crack length was a critical factor in the instability and propagation of fissures. Surface hardness varied with surface damage type. The presence of blistering or cracking altered hardness values, revealing changes in the mechanical properties of the surface. Wave velocity was closely associated with the internal structure and elastic modulus of the rock. Wave velocity was sensitive to subsurface cracks and cavities and served as a robust indicator of overall rock mass quality.

Pairwise comparisons of these indicators were performed using a standardized nine-point scale (Table 6). The random consistency index (RI) values are listed in Table 7. The resulting AHP judgment matrix and corresponding eigenvalues are summarized in Tables 8 and 9, respectively. The maximum eigenvalue was 4.248, with a consistency index (CI) of 0.083, yielding a CR of 0.093 (Table 10). This was below the accepted threshold of 0.1, demonstrating the reliability and consistency of the judgment matrix.

The weights assigned to the indicators revealed that crack length had the greatest significance (55.9%), followed by surface hardness (21.4%), wave velocity (16.0%), and surface thickness (6.8%). The measured values of each indicator for the three deterioration types are presented in Table 11. The data were normalized to ensure comparability (Table 12). Quantitative stability scores were derived from the calculated weights and normalized values (Table 13). Among the deterioration forms analyzed, splitting exhibited the highest instability score (0.720), indicating that it was the most active and hazardous condition, followed by blistering (0.149) and delamination (0.131).

3.4 Comprehensive Damage Assessment

FCE was used to integrate the deterioration impact and stability indices into a single comprehensive damage assessment. Three deterioration types—blistering, splitting, and delamination—were evaluated. The criteria considered in the analysis comprised qualitative descriptions of impact severity and the corresponding quantitative indices (Table 14).

The combined datasets for impact and stability indices for each deterioration type are presented in Table 15. These values were used to construct the fuzzy evaluation matrix. Membership degrees and normalized weights were obtained based on the analysis (Table 16). The normalized weights indicated that splitting (0.440) had the highest overall damage contribution, followed by delamination (0.418) and blistering (0.142). According to the principle of maximum membership degree, splitting represented the most critical type of deterioration in terms of the current damage risk.

4. DISCUSSION

4.1 Interpretation of In-Situ Nondestructive Physical Property Measurements

The comprehensive results obtained from in-situ NDT offered critical insights into the weathering deterioration mechanisms of Helankou rock art. Leeb hardness testing revealed significant decreases in surface hardness in blistering and splitting zones, which were attributable to internal voids and fissures compromising the structural integrity of the rock. The decreased rebound velocity observed in these regions showed that impact energy dissipated within the weakened matrix, indicating active mechanical degradation. Conversely, the lower hardness values in post-delamination subsurface areas reflected increased surface

Table 6 Nine-Point AHP Scale

Scale	Relative Importance
1	Two factors are of equal importance
3	One factor is slightly more important than the other
5	One factor is more important than the other
7	One factor is significantly more important than the other
9	One factor is extremely more important than the other
2, 4, 6, 8	Intermediate values between the above judgments

Table 8 AHP Judgment Matrix for Deterioration Stability Indicators

Indicator (Criterion)	Surface Thickness	Crack Length	Surface Hardness	Wave Velocity
Surface Thickness	1	1/5	1/4	1/3
Crack Length	5	1	5	3
Surface Hardness	4	1/5	1	2
Wave Velocity	3	1/3	1/2	1

Table 7 RI Values

Matrix Order (n)	1	2	3	4	5	6	7	8	9
RI	0	0	0.52	0.89	1.12	1.26	1.36	1.41	1.46

Table 9 AHP Results: Eigenvalues and Weights of Stability Indicators

Indicator	Priority Vector (Normalized Eigenvector)	Weight (%)	Max Eigenvalue	CI Value
Surface Thickness	0.359	6.821	4.248	0.083
Crack Length	2.943	55.865		
Surface Hardness	1.125	21.350		
Wave Velocity	0.841	15.963		

Table 10 Consistency Check Results of the AHP Matrix

Max Eigenvalue	CI	RI	CR	Consistency Judgment
4.248	0.083	0.890	0.093	Passed

Table 11 Measured Values of Stability Indicators by Deterioration Type

Indicator	Blistering	Splitting	Delamination
Surface Thickness	5 mm	9 mm	5 mm
Crack Length	0 mm	17 mm	0 mm
Surface Hardness	$(535)^{-1}$ HLD	$(535)^{-1}$ HLD	$(569)^{-1}$ HLD
Wave Velocity	3918.1 m/s	3918.1 m/s	2965.8 m/s

Table 12 Normalized Values of Stability Indicators

Indicator	Blistering	Splitting	Delamination
Surface Thickness	0.25	0.4	0.35
Crack Length	0.00	1.00	0.00
Surface Hardness	0.34	0.34	0.32
Wave Velocity	0.36	0.36	0.27

Table 13 AHP Results: Quantitative Evaluation of Deterioration Stability

Deterioration Type	Quantitative Stability Index
Blistering	0.149
Splitting	0.720
Delamination	0.131

Table 14 Criteria for Comprehensive Damage Assessment of Helankou Rock Art

Deterioration Type	Impact Severity (Qualitative)	Impact Index (Quantitative)
Blistering	Somewhat Severe	0.065
Splitting	Severe	0.163
Delamination	Very Severe	0.772

Table 15 Input Dataset for FCE

Indicator	Blistering	Splitting	Delamination
Impact Index	0.065	0.163	0.772
Stability Index	0.149	0.72	0.131

Table 16 Membership Degrees and Normalized Weights of Deterioration Types

Parameter	Blistering	Splitting	Delamination
Membership Degree	0.214	0.663	0.631
Normalized Weight	0.142	0.44	0.418

roughness of freshly exposed rock rather than intrinsic mechanical weakening. This distinction is crucial for conservation prioritization, as it differentiates ongoing deterioration from stabilized historical damage.

Cavities in deteriorated surfaces hinder heat transfer, resulting in elevated surface temperatures, particularly under high ambient temperatures, as observing during summer testing. Furthermore, these voids act as moisture reservoirs during precipitation events, increasing the surface moisture content and facilitating deleterious processes, such as freeze–thaw cycles and salt crystallization. The observed heterogeneity between surface and subsurface moisture levels underscores the complex microenvironmental factors that affect weathering progression. These interacting effects collectively form a positive feedback mechanism that accelerates physical degradation, indicating that conservation strategies must address both visible surface deterioration and underlying environmental influences.

Moreover, the strong positive correlation between QI_i values and deterioration coverage suggests that QI_i is a robust quantitative proxy for internal void content and structural damage.

4.2 Interpretation of Static and Dynamic Characteristics of Deterioration

This study developed a dynamic deterioration model using static morphological data to describe the temporal evolution of weathering in Helankou rock art. This model delineated three stages: (1) initial stage with intact appearance and latent primary fissures; (2) development stage featuring progressive fissure propagation, void formation (blistering), and visible splitting; and (3) final stage characterized by surface delamination, irreversible layer detachment, and severe loss of cultural information. This dynamic framework underscores the cumulative and irreversible nature of sandstone weathering and provides a basis for interpreting current conditions and future trajectories of deterioration.

This analysis demonstrated that blistering and splitting represented the most unstable forms of deterioration, which was consistent with their developmental stage status. In particular, splitting reflected a state of high instability due to stress concentration at fissure tips, which promoted rapid crack propagation and accelerated surface fragmentation. In contrast, delamination, despite being visually more destructive, represented a post-failure stage with detached unstable layers releasing accumulated stresses and leaving behind stable fresh surfaces.

4.3 Interpretation of the Quantitative Assessment of Deterioration Stability

Implementing the AHP provided a rigorous and structured framework for quantitatively evaluating the stability of the types of deterioration affecting Helankou rock art. The results identified splitting as the most unstable form of deterioration, whereas blistering and delamination were less critical. This ranking aligns with the proposed deterioration evolution model, in which splitting and blistering represent dynamic progressive damage processes that threaten the integrity of the rock surface. The reliability of this evaluation was supported by the consistency ratio, which confirmed the methodological soundness of the judgment matrix.

Unlike conventional surveys of sandstone deterioration, which primarily document static morphological features, such as exfoliation thickness and visible surface loss, the AHP-based framework incorporates stability as a dynamic parameter. This approach characterizes the current state of deterioration and provides insights into its future trajectory. This perspective is essential for preventive conservation, as it aids the prioritization of monitoring and intervention before irreversible loss of rock art information.

4.4 Comprehensive Damage Assessment and Implications for Conservation

FCE integrated quantitative deterioration impact and stability indices of three major deterioration types—blistering, splitting, and delamination—and yielded a holistic assessment of current damage risk. The normalized weights indicated that splitting contributed the most to overall damage, followed by delamination and blistering. This indicates that splitting represents the predominant threat, despite delamination causing the most visible loss.

This distinction highlights the importance of prioritizing the proactive mitigation of dynamically evolving deterioration over the reactive treatment of visually apparent damage. The higher risk associated with splitting is consistent with its developmental stage, which is characterized by active fissure propagation and local bulging. Conversely, delamination reflects the final stage of weathering with a comparatively stabilized substrate.

5. CONCLUSION

This study conducted a comprehensive quantitative assessment of the deterioration of Helankou rock art by integrating in-situ NDT with multi-criteria analysis. The findings revealed that internal voids and fissures significantly affected key physical parameters, comprising surface hardness, temperature, moisture content, and ultrasonic wave velocity, in areas affected by splitting and blistering. The presence of these structural defects, coupled with thermal and moisture anomalies, exacerbated deterioration due to thermomechanical stresses and moisture-driven processes.

Quantitative multicriteria analysis identified splitting as the most unstable and hazardous form of deterioration, highlighting its critical role in the rapid degradation of rock art. This underscores the urgent need to prioritize conservation efforts focusing on active deterioration processes rather than merely addressing visually apparent damage. The dynamic deterioration development model proposed in this study provides a scientifically robust framework for predicting the progression of rock art weathering.

These results offer actionable guidance for conservation. Intensive monitoring and preventive interventions should primarily target splitting, whereas blistering can serve as an effective diagnostic indicator of early-stage risk detection. Considering its high instability and contribution to accelerated surface loss, timely reinforcement and stabilization measures are strongly recommended for splitting-induced deterioration.

This study advances the scientific understanding of rock art degradation and provides practical data-driven tools for cultural heritage preservation. Nevertheless, the indicator system used in this study was developed based on the available field data and should be regarded as preliminary. Although these indicators capture the key aspects of surface and subsurface conditions, they do not fully account for critical factors such as permeability, strength heterogeneity, microstructural anisotropy, and mineralogical alterations induced by weathering. This limits the comprehensiveness of the assessments. This framework should be refined by expanding field investigations and incorporating additional parameters to establish a robust stability-based model for evaluating weathering deterioration in cultural heritage contexts. Continued multi-seasonal environmental monitoring and advanced nondestructive diagnostic techniques should be used to improve early detection and facilitate targeted conservation interventions. This integrative approach provides a solid foundation for the sustainable preservation of Helankou rock art and offers a replicable methodology for research on and conservation of similar cultural heritage sites worldwide.

FUNDING

This work was supported by the Ningxia Hui Autonomous Region Bureau of Cultural Relics under the project “Preliminary Survey and Research on the Protection of Helan Mountain Rock Paintings” (grant number Ningwenwufa No. 83), spanning from July 2021 to March 2026. We also thank the Yinchuan Municipal Administration of Helan Mountain Rock Art, 199 East Square Road, Yinchuan, Ningxia, China, for their assistance during field investigations.

REFERENCES

Bodnar, J. L., Candoré, J. C., Nicolas, J. L., Szatanik, G., Detalle, V., & Vallet, J. M. (2012). Stimulated infrared thermography applied to help restoring mural paintings. *NDT & E International*, *49*, 40-46. https://doi.org/10.1016/j.ndteint.2012.03.007

Dario Camuffo. (2018). Standardization activity in the evaluation of moisture content. *Journal of Cultural Heritage*, *31*, S10-S14. https://doi.org/10.1016/j.culher.2018.03.021

Davin, T., Serio, B., Géraldine, G., & Pina, V. (2017). Spatial resolution optimization of a cooling-down thermal imaging method to reveal hidden academic frescoes. *International Journal of Thermal Sciences*, *112*, 188-198. https://doi.org/10.1016/j.ijthermalsci.2016.10.007

Desarnaud, J., Kiriyama, K., Bicer Simsir, B., Wilhelm, K., & Viles, H. (2019). A laboratory study of Equotip surface hardness measurements on a range of sandstones: What influences the values and what do they mean? *Earth Surface Processes and Landforms*, *44*(7), 1419-1429. https://doi.org/10.1002/esp.4584

Fitzner, B., Heinrichs, K., & Bouchardiere, D. (2004). The Bangudae Petroglyph in Ulsan, Korea: Studies on weathering damage and risk prognosis. *Environmental Geology*, *46*, 504-526. https://doi.org/10.1007/s00254-004-1052-x

Fitzner, B., Heinrichs, K., & Bouchardiere, D. L. (2002). Damage index for stone monuments.

Fitzner, B., Heinrichs, K., & Bouchardiere, D. L. (2003). Weathering damage on Pharaonic sandstone monuments in Luxor-Egypt. *Building and Environment*, *38*(9), 1089-1103. https://doi.org/10.1016/S0360-1323(03)00086-6

Fitzner, B., Heinrichs, K., & Kownatzki, R. (1997). Weathering forms at natural stone monuments—Classification, mapping and evaluation. *Restoration of Buildings and Monuments*, *3*. https://doi.org/10.1515/rbm-1997-0204

Fourmaintraux, D. (1975). Quantification des discontinuités des roches et des massifs rocheux. *Rock Mechanics*, *7*(2), 83-100. https://doi.org/10.1007/BF01351903

Huo, X., Ma, R., & Ma, E. (2024). Weathering diseases characteristics and impact assessment of helankou rock art. *Journal of Rock Art*, *3*(1), 09–19.

Leucci, G., & Giorgi, L. D. (2022). Integrated ndt for building cultural heritage. *In Handbook of Cultural Heritage Analysis*, 739-769. Springer, Cham. https://doi.org/10.1007/978-3-030-60016-7_26

Menningen, J., Siegesmund, S., Tweeton, D., & Träupmann, M. (2018). Ultrasonic tomography: non-destructiv evaluation of the weathering state on a marble obelisk, considering the effect of structural properties. *Environmental Earth Sciences*, *77*. https://doi.org/10.1007/s12665-018-7776-9

Olson, D. L. (1996). The analytic hierarchy process. In D. L. Olson (Ed.), *Decision Aids for Selection Problems*, 49-68. Springer. https://doi.org/10.1007/978-1-4612-3982-6_5

Pappalardo, G. (2015). Correlation between p-wave velocity and physical–mechanical properties of intensely jointed dolostones, peloritani mounts, ne sicily. *Rock Mechanics and Rock Engineering*, *48*(4), 1711-1721. https://doi.org/10.1007/s00603-014-0607-8

Randazzo, L., Collina, M., Ricca, M., Barbieri, L., Bruno, F., Arcudi, A., & Russa, M. L. (2020). Damage indices and photogrammetry for decay assessment of stone-built cultural heritage: The case study of the san domenico church main entrance portal (south calabria, italy). *Sustainability*, *12*, 5198. https://doi.org/10.3390/su12125198

Siedel, H., & Siegesmund, S. (2014). Characterization of stone deterioration on buildings. In S. Siegesmund & R. Snethlage (Eds.), *Stone in Architecture: Properties, Durability*, 349-414. Springer. https://doi.org/10.1007/978-3-642-45155-3_6

Siegesmund, S., Menningen, J., & Shushakova, V. (2021). Marble decay: Towards a measure of marble degradation based on ultrasonic wave velocities and thermal expansion data. *Environmental Earth Sciences*, *80*. https://doi.org/10.1007/s12665-021-09654-y

Si-jian, Q., Ze-ping, Y., Hai-an, L., Yi-dong, M., Fu-jun, L., & Guang-yang, H. (2021). *Experimental Study on Uniaxial Compressive Strength of Danxia Formation Clastic Rocks in Northern Guangdong Based on N-type Schmidt Hammer*. *7*.

Tejedor Herrán, B., Bienvenido-Huertas, D., Lucchi, E., & Nardi, I. (2024). A comprehensive overview of NDT: From theoretical principles to implementation. *Diagnosis of Heritage Buildings by Non-Destructive Techniques*, 3-20. https://doi.org/10.1016/B978-0-443-16001-1.00001-2

Wilhelm, K., Viles, H., & Burke, Ó. (2016). Low impact surface hardness testing (Equotip) on porous surfaces-advances in methodology with implications for rock weathering and stone deterioration

research: Equotip Hardness Testing on Porous Rock and Stone. *Earth Surface Processes and Landforms*, *41*(8), 1027-1038. https://doi.org/10.1002/esp.3882

Xu, X., Ran, B., Jiang, N., Xu, L., Huan, P., Zhang, X., & Li, Z. (2024). A systematic review of ultrasonic techniques for defects detection in construction and building materials. *Measurement*, *226*, 114181. https://doi.org/10.1016/j.measurement.2024.114181

Xu, X., Yu, F., Pedrycz, W., & Du, X. (2023). Multi-source fuzzy comprehensive evaluation. *Applied Soft Computing*, *135*, 110042. https://doi.org/10.1016/j.asoc.2023.110042

Young-Jun, Lee., Young-Seuk, Keehm., Min-Hui, Lee., June-Hee, Han., & Min-Su, Kim. (2012). Assessment and calibration of ultrasonic velocity measurement for estimating the weathering index of stone cultural heritage. *Journal of the Korean Earth Science Society*, *33*, 126-138. https://doi.org/10.5467/JKESS.2012.33.2.126